EXPERIMENTAL INVESTIGATION OF INSTALLATION EFFECTS IN A LOW-SPEED FAN SYSTEM

Joachim DOMINIQUE[1], Julien CHRISTOPHE[1],
Raul CORRALEJO[2], Christophe SCHRAM[1]

[1] *von Karman Institute, Bruxelles, Rhodes-St-Genese, 1640, Belgium* [2] *Dyson Ltd,*

Tetbury Hill, SN16 0RP Malmesbury, England

SUMMARY

The integration of a fan inside a circuit as found in HVAC or household appliance applications causes an increase in noise levels compared to when the fan is tested as an isolated component. Using the multi-ports methodology, it is possible to separate the effects related to the acoustic wave propagation and scattering from the changes in the sound production of the fan due to non-uniform ingested flow. In this work, experimental multi-ports eduction results are compared to ISO measurements. Grids are later added upstream of the fan to perturb the uniformity of the ingested flow. The different grids and their influence on the acoustics power spectral density highlight the effects of flow uniformity on the noise produced by the fan.

INTRODUCTION

The thriving interest of customers and the ever-increasing regulations on the noise generated in domestic appliances, air-conditioning and cooling systems have increased the need for characterization and noise reduction techniques. This requires an improved understanding of aeroacoustic mechanisms, in particular of the interactions taking place between the components of HVAC systems or household appliances.

In-duct fan noise is usually characterized under uniform inflow profile even though such conditions are rarely met in practice due to product compactness and integration constraints. This leads to changes in the noise quality of the equipment that can compromise its acoustic performances and requires additional and expensive experimental prototyping. The influence of non-ideal installation on fan acoustic performance is called *the installation effects* and constitutes the purpose of the research presented below.

Installation effects are threefold. First, the non-uniformity of the flow ingested by the fan and its turbulence affect the unsteady rotating forces acting on the blades which are the dominant source of noise for fan at low tip Mach number [1]. Second, the installation of a fan within a circuit can also force the fan into off-design operations which cause changes in its aerodynamic performances [2].

Finally, the acoustic radiation efficiency of the duct terminations affects the perception of the noise emitted within the duct, which is a purely acoustical propagation effect [3].

It is possible to remove the influence of those acoustical scattering effects, by using the *multi-ports methodology* [4]. This technique, implementing arrays of loudspeakers and microphones, is used to discriminate between aerodynamic and acoustic effects and therefore allows to investigate the aerodynamic installation effects alone. Later, similitude laws are employed to respectively quantify the influence of change in the fan performances and more subtle aerodynamic installation effects.

This work consists in an investigation of the installation effects in a small air-moving device provided by Dyson Ltd using multi-ports eduction in the dedicated von Karman Institute wind tunnel ALCOVES (Fig. 1.b). Grids are used upstream of the fan to condition the flow and force the fan to operate in non-ideal working conditions. The effects of those off-design conditions on the aerodynamic and acoustic performances are evaluated for multiple grids.

The experimental setup is shown in Fig. 1.a. The facility consists of a duct of 15 cm diameter including two arrays of 12 loudspeakers and 13 Brüel and Kjær microphones on both sides of the fan. An adaptive module of smaller diameter was designed to fit the fan (Fig. 1.c) to the current facility. To ensure that the flow distortions generated by the grids reach the fan, the grids are installed in the adaptive module, upstream of the fan, at a distance of two diameters .

a) Experimental facility
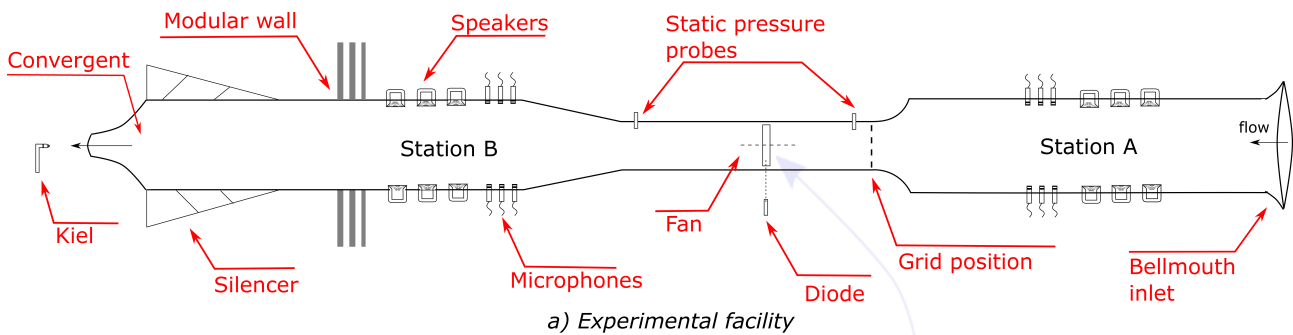
b) ALCOVES wind tunnel

c) Dyson Ltd fan

Figure 1: *Experimental facility of the von Karman Institute and the Dyson Ltd fan.*

ACOUSTIC MULTI-PORTS EDUCTION TECHNIQUE

Modal decomposition

Ducts have a specific way of propagating sounds since their confined environment acts as acoustic waveguides. By solving the Helmholtz equation, it can be shown that the acoustic field propagates with specific, self-similar shapes along the duct. Those represent elementary solutions, also called modes, of the acoustic field. Altogether, those modes form a base from which any solutions can be reconstructed. They act as building blocks to represent more complex phenomena.

At a given frequency, only a finite number of modes, for which the wave number $k_{m\mu}$ is real, are propagating inside the duct (m and μ being respectively the number of azimuthal and radial modes). For example, at low frequency, only the plane wave is propagating. More modes are progressively added when the frequency reaches the limits at which their respective $k_{m\mu}$ becomes real. Those frequencies are named the cut-on frequencies $f_{m\mu}$.

For constant cross section ducts, the acoustic pressure field can be represented as a sum of modes, either cut-on or cut-off in Eq. (1) [5]:

$$p(r, \theta, z) = \sum_{m=0}^{\infty} \sum_{\mu=0}^{\infty} U_{m\mu}(r) \left(\hat{p}_{m\mu}^+ e^{-ik_{m\mu}z} + \hat{p}_{m\mu}^- e^{ik_{m\mu}z} \right) e^{-im\theta} \qquad (1)$$

Where: $\quad U_{m\mu}(r) = N_{m\mu} J_m(\alpha_{m\mu}r), \quad N_{m\mu} = \left(\frac{1}{2} \left(1 - \frac{m^2}{\alpha_{m\mu}^2} \right) J_m(\alpha_{m\mu})^2 \right)^{-1/2},$

$$k_{m\mu}^{\pm} = \omega \left[\frac{\sqrt{1 - \left(\frac{\alpha_{mn}}{\omega} \right)^2 (1 - M^2)} \mp M}{1 - M^2} \right]$$

In those equations, J_m denotes a Bessel function of the first type that satisfies the boundary conditions at the hard wall and $\alpha_{m\mu}$ is the μth non trivial zero of the derivative of J_m. Finally, the wavenumber $k_{m\mu}$ is defined to account for the presence of mean flows [6].

Considering only N cut-on modes, Eq. (1) has $2N$ unknowns. Therefore, $2N$ microphones around one location in a duct provides a closed set of equations that permits the retrieval of the amplitudes experimentally for the left- and right-going waves for each of the N modes: $\hat{p}_{m\mu}^+$ and $\hat{p}_{m\mu}^-$. This can also be written in matrix form using the following convention:

$$\mathbf{P} = \mathbf{J}\mathbf{P}^{\pm} \qquad (2)$$

The multi-ports technique uses this modal description of the acoustic field to provide a black box analysis of a ducted component. Let's consider a fan connected to a straight duct system that includes loudspeakers and microphones arrays upstream and downstream as shown in Fig. 2.
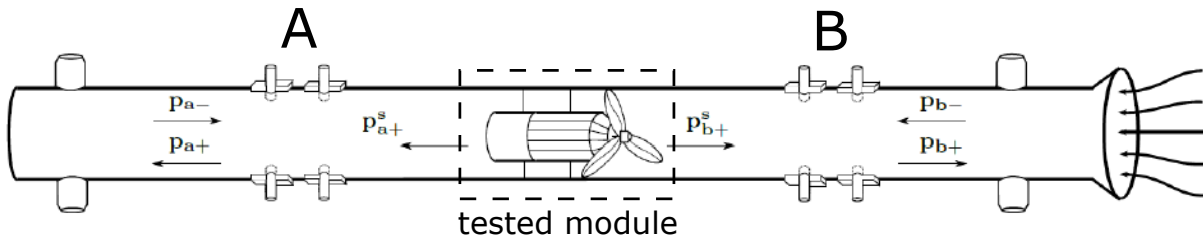
Figure 2: Schematic of the multi-ports method.

If the system can be considered as time-invariant, in the case of a plane wave, the wave going away from the source in A, called p_a^+, can be seen as the superposition of three components:

- The reflected part of the wave going toward the source in A: $\rho_a p_a^-$

- The transmitted part of the wave going toward the source in B: $\tau_a p_b^-$

- The acoustic wave produced by the source in the same direction: p_{a+}^s

Two of those components result from the scattering of the acoustic field across the source while the last one describes the noise production of the source. The same decomposition can be made on the other side of the source for p_b^+. This results in the following set of equations:

$$
\begin{aligned}
p_a^+ &= \rho_a p_a^- + \tau_a p_b^- + p_{a,+}^s \\
p_b^+ &= \rho_b p_b^- + \tau_b p_a^- + p_{b,+}^s
\end{aligned}
\tag{3}
$$

Where ρ and τ are respectively the reflection and transmission coefficient of the plane wave on the tested module. Generalizing this formulation to higher modes, Eq. (3) can be written in matrix from and the active noise generated by the studied module can be evaluated using [7]:

$$
\mathbf{P}^+ = \mathbf{S}\mathbf{P}^- + \mathbf{P}^s
\tag{4}
$$

Where $\mathbf{P}^+$ and $\mathbf{P}^-$ are the vectors that encompass the left- and right-going acoustic waves at the two microphones stations A and B. $\mathbf{S}$ is the scattering matrix of the tested module and describes the reflection and transmission coefficients of the different modes through the module. This formulation permits the extraction of the acoustic field produced by the sources within the module investigated ($\mathbf{P}^s$) without the scattering effects of the duct that would contaminate the acoustic measurements otherwise.

Experimental methodology

The methodology employed in this work for the multi-ports method seeks to retrieve the two unknowns from Eq. (4): $\mathbf{S}$ and $\mathbf{P}^s$. This requires two sets of experiments named *the active part* and *the passive part*.

The flowchart methodology used during this campaign is given in Fig. 3 and relies on the modal decomposition based on Eq. (1).
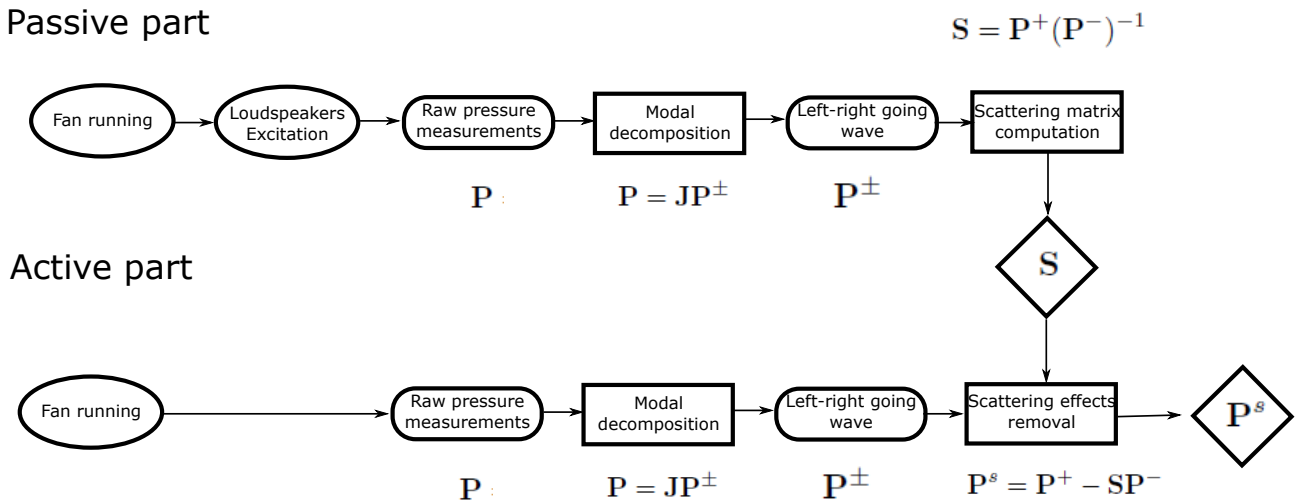
Figure 3: Flowchart of the experimental process.

The first experiment, *the passive part*, is used to evaluate the scattering matrix of the module. Loudspeakers are used to produce a strong acoustic field inside the duct. If the excitation of the loudspeakers

is large compared to the noise of the fan, the modal decomposition of the microphones reading can be used to retrieve the scattering matrix as:

$$\mathbf{P}^+ = \mathbf{S}\mathbf{P}^- + \mathbf{P}^s \quad \overset{\text{with loudspeakers: } \mathbf{P}^s \ll \mathbf{P}^-, \mathbf{P}^+}{\Longrightarrow} \quad \mathbf{S} \approx \mathbf{P}^+ \left(\mathbf{P}^-\right)^{-1} \tag{5}$$

In order to compute the scattering matrix $\mathbf{S}$, an additional numerical aspect has to be considered: $\mathbf{P}^-$ has to be inverted. Unfortunately, Eq. (5) has more unknowns than equations since $\mathbf{S}$ is $[2N \times 2N]$ while $\mathbf{P}^+$ and $\mathbf{P}^-$ are $[N \times 1]$. Therefore, additional equations must be considered to close the system. In the scope of an experimental work this can be done by taking additional independent measurements given by different loudspeaker locations, also called loadcases. Using 2N independent loadcases, $\mathbf{P}^-$ and $\mathbf{P}^+$ vectors are transformed into square invertible matrices.

It is clear that the computation of the scattering matrix is numerically heavy since 2N loadcases are required for each tested frequency. This can lead to large test matrices and long acquisition times. To fasten the acquisition process, two methods have been used. First, using specific hardware, it is possible to test 4 different loadcases simultaneously by exciting 4 different frequencies at once. Second, instead of measuring the scattering matrix for every single frequency, the scattering matrix is computed at specific frequencies and later interpolated to the all the frequencies of interest. This interpolating method cannot be used across the the cut-on frequencies due to change in size of $\mathbf{S}$. Therefore, the frequencies in those regions are badly resolve. However, this is not necessarily a problem since the multi-ports methodology is less accurate in those region due to bad conditioning of the matrices $\mathbf{J}$.

In the second experiment, *the active part*, the loudspeaker's excitation is turned off. The modal decomposition on the raw measurements represents the noise propagating in the duct due to the fan and the scattering effects. Those can be removed using the scattering matrix obtained in the passive part using :

$$\mathbf{P}^s = \mathbf{P}^+ - \mathbf{S}\mathbf{P}^- \tag{6}$$

Acoustic power

According to Myer's development [8], in an irrotational, isentropic flow, the acoustic energy is a conserved quantity. The acoustic power through a surface A with normal $\mathbf{n}$ can be computed as:

$$P = \int_A <\mathbf{I}.\mathbf{n}> dS \quad \text{with the intensity} \quad \mathbf{I} = \left(\rho_0 \mathbf{v}' + \rho' \mathbf{v}_0\right)\left(\frac{p'}{\rho_0} + \mathbf{v}_0.\mathbf{v}'\right)$$

Introducing the modal description of the acoustic pressure and velocity in a duct introduced in Eq. (1), the axial power across the duct section becomes [5]:

$$P = \pi\beta^4 \sum_{\text{cut-on}} \left[\frac{\sigma^+_{m\mu}|\hat{p}^+_{m\mu}|^2}{(1 - M\sigma^+_{m\mu})^2} + \frac{\sigma^-_{m\mu}|\hat{p}^-_{m\mu}|^2}{(1 - M\sigma^-_{m\mu})^2}\right]$$
$$+ 2\pi\beta^4 \sum_{\text{cut-off}} \frac{\tau_{m\mu}}{(1 + M^2\tau^2_{m\mu})^2} \left[(1 - M^2\tau^2_{m\mu})Im(\hat{p}^+_{m\mu}\bar{\hat{p}}^-_{m\mu}) - 2M\tau_{m\mu}Re(\hat{p}^+_{m\mu}\bar{\hat{p}}^+_{m\mu})\right] \tag{7}$$

$$\text{Where} \quad \beta = \sqrt{1 - M^2} \quad, \quad \sigma^\pm_{m\mu} = \pm\sqrt{1 - \left(\frac{\alpha_{m\mu}\beta}{\omega}\right)^2} \quad \text{and} \quad \tau_{m\mu} = i\sigma^+_{m\mu} = -i\sigma^-_{m\mu}.$$

The second term of Eq. (7) describes the influence of the cut-off modes on the acoustics power prop-agating inside the duct, which only contributes through interactions between left- and right-going modes. However, given that cut-off modes decrease exponentially, the product between the two is usually considered negligible. In practical applications, this term is often neglected [9].

When measuring the acoustic power from the multi-ports methodology using Eq. (6), it is important to remember that P_s describes the noise source *as if* it was in an infinite duct. In that context, the terms including $\hat{p}_{m\mu}^+$ describes the power propagating upstream of the source and $\hat{p}_{m\mu}^-$ the one downstream.

INSTALLATION EFFECTS INVESTIGATION

Fan noise under uniform inflow condition

Using the methodology previously described, the noise emitted by the Dyson fan was first evaluated under uniform inflow profile. The initial raw measurements are obtained before the application of the multi-ports technique (Fig. 4, blue curve). They are contaminated by turbulent pressure fluctuations of the wall boundary layer and acoustic scattering effects (this includes reflections on the duct terminations, standing waves, etc). Once the modal decomposition is performed, the results can be used to reconstruct an image of the initial measurements (red curve). Since this image was obtained by a fitting of the experimental results to a theoretical solution of the acoustic field inside the duct, it does not account for turbulent pressure fluctuations. The small differences between the raw and the reconstructed signals indicates that, at such small volume flow rate, the turbulent boundary layer pressure fluctuations affect very little the microphone's signal.
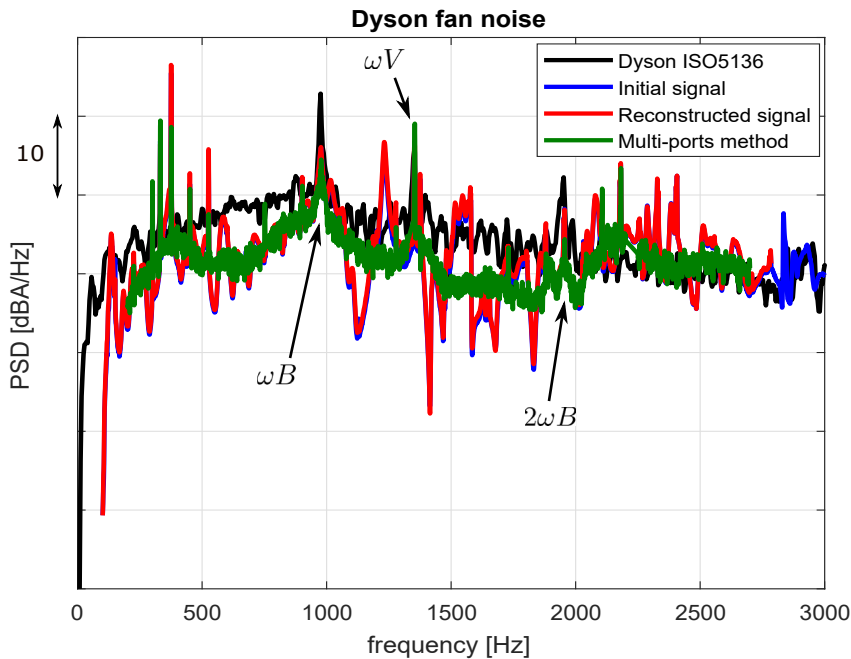
Figure 4: Power spectral density of the Dyson Ltd fan noise from the multi-ports eduction technique and ISO-5136 at similar flow rate.

The green curve corresponds to the results obtained after applying the multi-ports eduction on the initial measurements. It appears to have removed most of the large amplitude oscillations that were likely caused by constructive/destructive interferences from acoustic standing waves within the duct. Figure 4 also shows independent results performed by Dyson on a different setup using the ISO-5136 methodology [10]. Globally, the two spectra obtained are in good agreement. They perfectly match

at high frequency, but lower amplitudes are observed in the low to mid-frequency range. A thorough comparison between the two spectra can be used to show that the same physics is represented.

The Ffowcs Williams and Hawkings analogy [11] states that the noise generated by fan can be decomposed into three main components: the thickness noise, the turbulence noise and the loading noise. At low Mach number and for thin rotor/stator blades, the unsteady loading noise dominates the sound production. This loading noise is characterized by a broadband and a tonal component. The latter is emitted at the blade passing frequencies $n\omega B$ (with B being the number of rotor blades) and produced by the unsteady forces acting on the blades [12]. The blade passing frequencies (BPF) are well identified in both ISO-5136 and multi-ports measurements.

An additional tonal peak at the frequency ωV (V being the number of stator vanes) is also captured in both measurement series. This peak is not explained by the Ffowcs Williams and Hawkings analogy, which clearly states that the tonal peaks should occur at the blade passing frequency regardless of the number of stator vanes. Such harmonic is likely driven by a perturbation similar to a single blade wake of periodicity 1 at the rotor interacting with the V stator vanes. This could be caused by a seperation at the hub or a non-uniformity in the rotor blades manufacturing. Unfortunately, the resulting peak frequency for this phenomenon also corresponds to the first cut-on frequency $f_{1,0}$ of the duct for which the conditioning of the modal decomposition is poor. It results that the amplitude measured by the multi-ports technique is likely miss-evaluated at this particular frequency.

Aerodynamic performance with installation effects

To generate installation effects, grids are used upstream of the fan to generate non-uniformity in the incoming flow. Those grids (Fig. 5) have been selected to induce large radial and azimuthal mean flow distortions ("Fractal" and "Half") and increase turbulence level ("Grid"). They are expected to modify the tonal and broadband content of the noise generated by the fan.
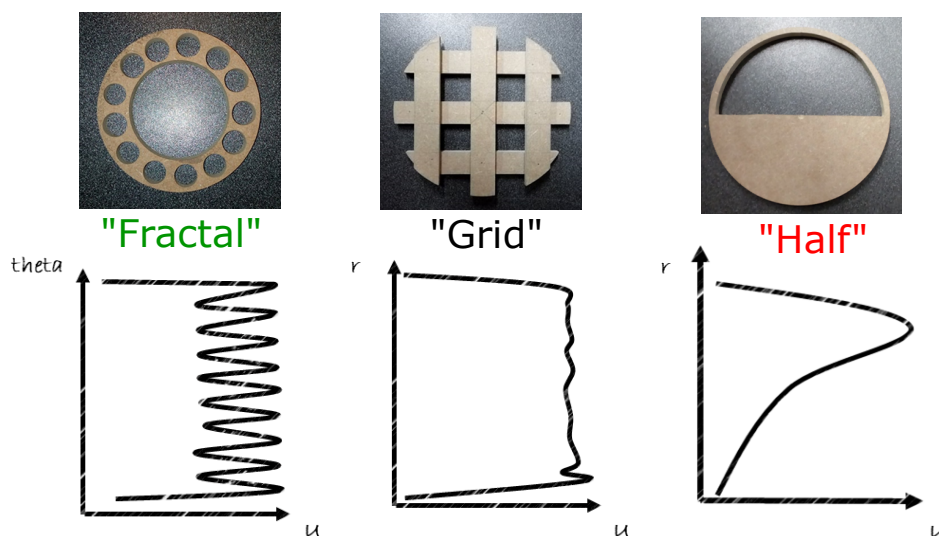
Figure 5: Distortion grids used to generate installation effects and corresponding expected inflow distortions downstream of the grid.

However, non-uniformities in the flow change the velocity triangle seen by the blades of the fan which in turns affect its aerodynamic performance [3]. Figure 6 shows how the performance curves of the fan are affected by the different distorted inflows. The performances of the fan ares evaluated using a Kiel probe at the rear of the duct to avoid the influence of swirl past the fan. The change in operating conditions of the fan was done by closing a butterfly valve situated in the exhaust circuit of the wind

tunnel which is not represented in Fig. 1. Finally, in order to account for the pressure losses in the duct, additional measurements performed without the fan are used to correct the total pressure measured by the Kiel probe.
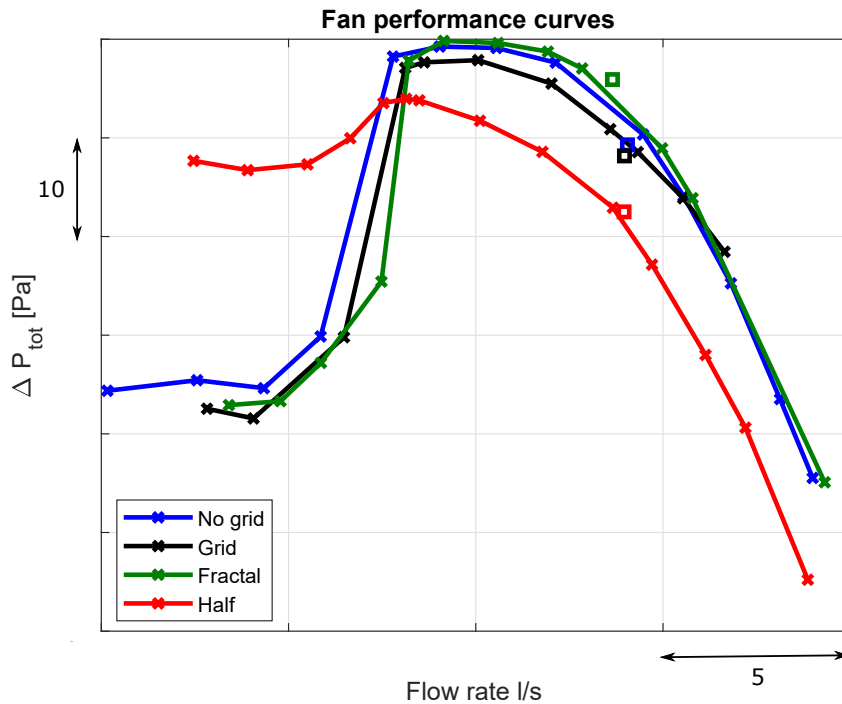
Figure 6: Effects of non-uniform inlet conditions on the fan performances. The square dots indicate the operating conditions used for the multi-ports eduction measurements.

As it can be seen in Fig. 6, when grids are added, the fan no longer works in ideal conditions. Its performances are thus reduced as it is illustrated by the drop in total pressure for the different obstructions. The "Grid" and "Fractal" configurations have limited effects on the fan performance and stall point. However, the "Half" grid showed important differences as the total pressure drops after the stall was less important than for the other grids.

This adds up to the complexity of the investigations of acoustic installation effects. Indeed, even though all the tests were performed at similar volume flow rate, the pressure rise of the fan differs depending on the grids installed inside the duct. Since pressure rise across a fan is a critical parameter of the noise it generates, it therefore matters to unveil if the acoustic installation effects observed are strictly due to changes in total pressure operating point or to more subtle effects.

To determine whether the changes in acoustic power observed are due to a modification of the fan operating point, a similarity law is used [2]:

$$W_2 = W_1 + 10log\left(\frac{Q_2}{Q_1}\right) + 20log\left(\frac{\Delta P_2}{\Delta P_1}\right) \tag{8}$$

This law, mainly used for design purposes, scales the acoustic power of a fan (W_2) from previous measurements (W_1) performed on the fan under uniform inflow condition at the same rotational speed. In Tab. 1, the prediction obtained using Eq. (7) is compared to the acoustic power measured for the different grids using.

It can be seen that the increase in noise power observed through Eq. (7) is completely different from what is obtained with the similarity law. Equation (8) only predicts small changes in the acoustic power

while the measured power levels are strongly increased depending of the obstruction considered. This shows that installation effects cannot be reduced to changes in the aerodynamic performances of the fan only. It also highlights that this similarity law is not well adapted to account for installation effects.

Obstruction	No grid	Fractal	Grid	Half
Acoustic Power Eq. (7) [dB]	W1 = 68.87 (+0)	72.73 (+3.86)	77.37 (+8.5)	83.5 (+14.63)
Similarity Eq. (8) [dB]	W1 = 68.87 (+0)	69.20 (+0.33)	68.79 (-0.08)	68.42 (-0.45)

Table 1: The acoustic power computed with Eq. (7) upstream of the fan for the different obstructions and their increment compared to the uniform flow case. The similarity is obtained with the fan performance conditions described by the square dots in Fig. 6.

Grids self-noise

Since the multi-ports methodology is a black-box measurement, the noise measured by the technique represents all the elements situated in-between the two microphones stations (i.e. the grids, the adaptive module and the fan).

To discuss the noise generated by the fan alone, it is essential to rank the importance of the noise generated by the other components. The multi-ports methodology (active and passive measurements) was applied on the module without the fan in Fig. 7. The self-noise of each obstruction is displayed and compared to the noise of the fan under uniform inflow.
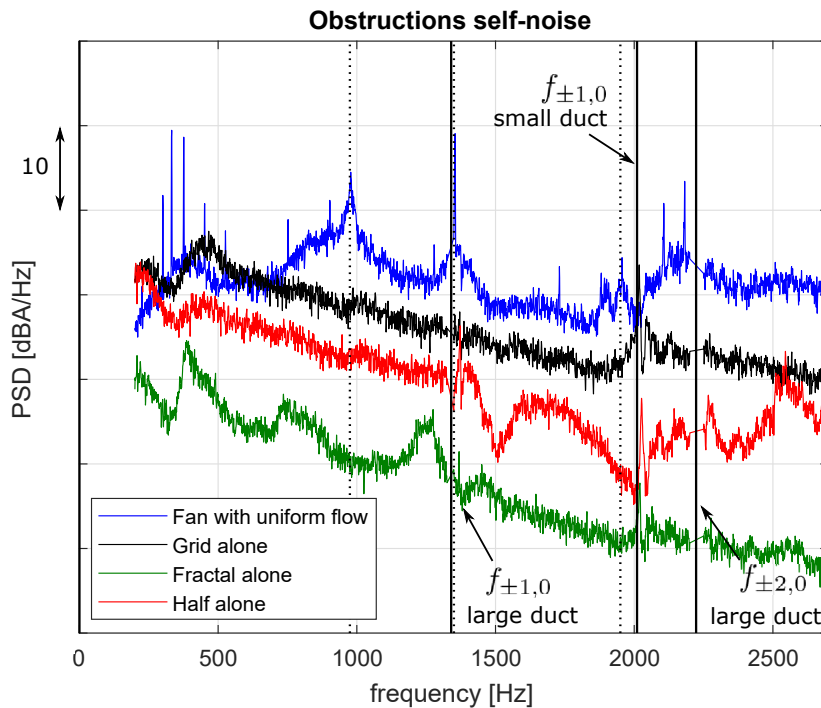
Figure 7: Power spectral density of the grids self-noise at the flow rate indicated by the square dots in Fig. 6. The vertical full lines represent the cut-on frequencies of the duct and the vertical dashed lines correspond to the blade passing frequencies and stator harmonic.

It can be seen that the noise of the grids alone within the duct is always lower than the noise of the fan except at low frequency. To avoid the possible corruption of the acoustic spectrum of the fan noise by grid self-noise, the latter was removed from the active measurements presented in next section.

Acoustic installation effects

Figures 8 and 9 show the power spectral density of the noise generated by the fan for upstream and downstream microphones after the multi-ports eduction is performed.

As expected, for all obstructions, the noise is increased compared to the uniform flow configuration. The obstruction set by the "Grid" increased the broadband noise by 10 dBA over the entire spectrum. In addition, the tonal peaks at the BPF and the stator harmonic no longer emerge from the broadband noise. However, it is possible that the tonal components are simply hidden within the increase of broadband noise.

The "Half" obstruction has the most important effects on the power spectral density. As in the "Grid" distortion, the broadband noise is raised by 14 dBA. Nevertheless, a strong and narrow tonal peak can still be observed at the first blade passing frequency. This indicates an increase in both the tonal and broadband noise.

The last obstruction named "Fractal" used B azimuthal distortions with as minimum blockage as possible. It was therefore expected to generate an increase in the tonal noise of the fan with limited broadband effect. Surprisingly, no tonal peaks can be observed. Also, the amplitude of the noise at high frequency seems to remain unchanged compared to the uniform flow case. This indicates no or little increase in broadband noise. However, a large frequency band increase can be seen around the first BPF. It should be noted that other attempts were made to generate tonal noise using different grids with B azimuthal distortion, but none of those obstructions led to significant tonal noise increase.

Noticeable differences can be seen between the downstream (Fig. 8) and upstream (Fig. 9) spectra. The tonal noise for the "Half" obstruction seems to be more strongly emerging from the spectrum downstream of the fan. The effects of the cut-on frequencies is also more marked as a clear increase in the amplitude can be observed after the first cut-on frequency of the small duct, when the first azimuthal modes start to propagate.

The results obtained for the "Grid" and "Half" configurations are indicators of how turbulence in the ingested flow affects the fan noise. Indeed, those are strong and disruptive obstructions that likely increased the turbulence and both were accompanied with an increase in broadband noise of more than 10 dB.

On the other hand, the lack of tonal noise increase in the "Fractal" configuration indicates that azimuthal distortions have no effect on the tonal noise for the considered fan design. However, it was observed in the "Half" configuration that tonal noise increase was possible. It is therefore likely that another flow mechanism is responsible for the tonal noise of the fan. For example, this last obstruction can be characterized by a local increase of the flow velocity on its open half section. Maybe the tonal noise is more affected by strong increase of flow velocity rather than small periodic perturbations. This is still under investigation.

CONCLUSION

In this study, three different obstructions were investigated using the multi-ports eduction technique to highlight the installation effects and their main driving parameters in a low speed axial fan application. The comparison with the results obtained using ISO-5136 measurements highlighted the validity of the methodology used in this project. In addition, it was shown that this method effectively removed the acoustical scattering effects of the duct that would have contaminated the microphone's signal otherwise. This makes the multi-ports eduction a powerful tool to investigate installation effects.

Non-uniformity in the flow always led to increased sound power level of the fan and decreased aero-
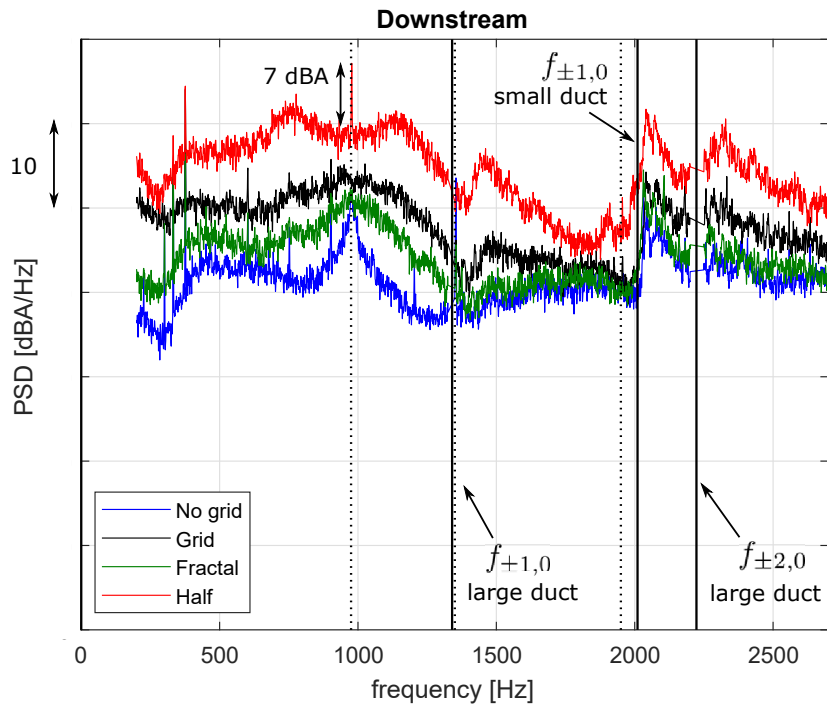
Figure 8: Acoustic installation effects for downstream microphones. The vertical full lines represent the cut-on frequencies of the duct and the vertical dashed lines correspond to the blade passing frequencies and stator harmonic.
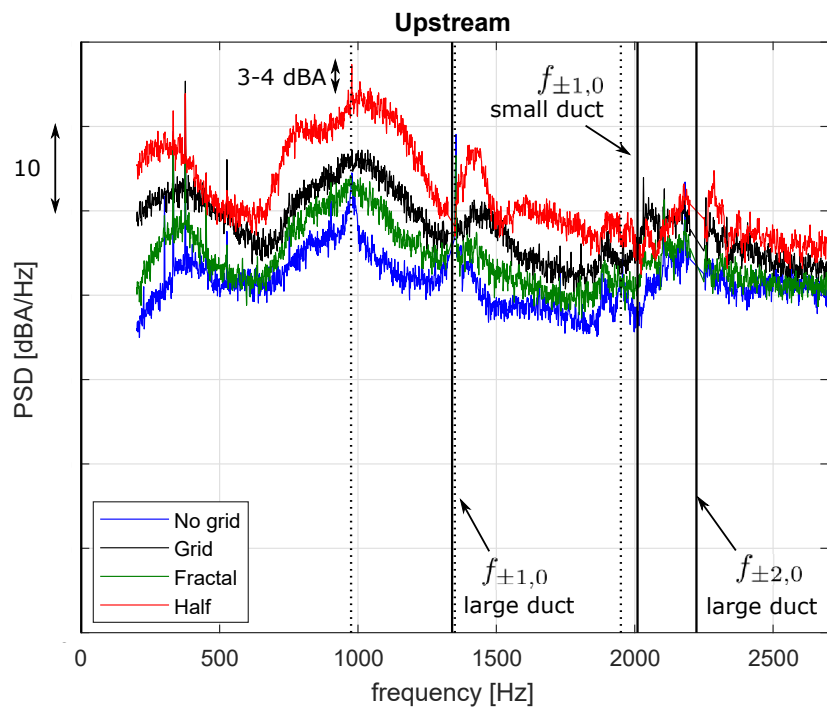
Figure 9: Acoustic installation effects for upstream microphones. The vertical full lines represent the cut-on frequencies of the duct and the vertical dashed lines correspond to the blade passing frequencies and stator harmonic.

dynamic performances. The most disruptive obstruction ("Half") caused the strongest fan noise power increase and performance change. Using similarity laws, it was shown that those aerodynamic performance changes alone were not sufficient to explain installation effects. Also, this highlighted that the similarity law used in this work was not adapted to account for the influence of installation effects.

The large obstructions, likely responsible for a turbulence increase, have a strong effect on the fan broadband noise, increasing the noise level up to 14 dB. In the "Grid" configuration, this large increase in broadband noise likely masked the tonal peaks at the BPF which are known to cause strong discomfort to the users.

A tonal noise increase was observed for the "Half" obstruction. But, surprisingly, the periodic azimuthal flow perturbations that were expected to affect the tonal peaks did not exhibit this foreseen behaviour. The lack of tonal peak in those configurations is interesting as it indicates that, maybe, another mechanism is responsible for the tonal noise production in this particular fan design.

REFERENCES

[1]   W. Neise. *Generation mechanisms and control method*. In *Fan noise*, Procedding of inter-noise 88, **1988**.

[2]   A. Guedel. *Generation du bruit et moyens de reduction*. In *Acoustique des ventilateurs*, CETITA, France, **1990**.

[3]   A. Bolton. *Installation effect on fan system*. In *National Engineering Laboratory*, National Engineering Laboratory, Germany, **1990**.

[4]   J. Lavrentjev and M. Abom. *Characterisation of fluid machines as acoustic multi-port sources*. Journal of Sound and Vibration, 197(1):1–16, **1996**.

[5]   S.W. Rienstra. *Uniform medium with mean flow*. In *Fundamental of duct acoustics,*, Technische Universiteit Eindhoven, Netherlands, **2015**.

[6]   L. Morfey. *Sound transmission and generation in ducts with flow*. Journal of Sound and Vibration, 14(1):37–55, **1971**.

[7]   W. De Roeck and C. Schram. *Integrated design of optimal ventilation systems for low cabin and ramp noise*. In *IDEALVENT Deliverable*, FP7 european project, **2016**.

[8]   M. Myers. *An exact energy corollary for homotropic flow*. Journal of Sound and Vibration, 2(109):277–284, **1986**.

[9]   H. Denayer. *Acoustic power dissipation and generation by multi-port elements*. In *Flow acoustic characterization of duct components using multi-port techniques*, KUL, Beligum, **2017**.

[10] ISO 5136. *Acoustics – Determination of sound power radiated into a duct by fans and other air-moving devices – In-duct method*, **2003**.

[11] J. E. Ffowcs Williams and D. L. Hawkings. *Sound Generation by Turbulence and Surfaces in Arbitrary Motion*. Philosophical Transactions of the Royal Society of London. Series A, Mathematical and Physical Sciences, 264(1151):321–342, **1969**.

[12] C. Schram. *Introduction to acoustics and aerocoustical analogies*. In *Aeroacoustics introduction*, Rhodes saint genese, Belgique, **2016**.